General Disclaimer

One or more of the Following Statements may affect this Document

- This document has been reproduced from the best copy furnished by the organizational source. It is being released in the interest of making available as much information as possible.

- This document may contain data, which exceeds the sheet parameters. It was furnished in this condition by the organizational source and is the best copy available.

- This document may contain tone-on-tone or color graphs, charts and/or pictures, which have been reproduced in black and white.

- This document is paginated as submitted by the original source.

- Portions of this document are not fully legible due to the historical nature of some of the material. However, it is the best reproduction available from the original submission.

Final Report

for the contract entitled

Development of Surfaces Optically Suitable for Flat Solar Panels
Contract No. NAS8-32481

prepared by

Donald De Smet
Andrew Jason
Albert Parr

and

Department of Physics and Astronomy
P. O. Box 1921
The University of Alabama
University, Alabama 35486

prepared for

George C. Marshall Space Flight Center
Marshall Space Flight Center, Alabama 35812

Abstract

This final report under NAS8-32481 contains three principal items. The first describes a simple and novel reflectometer which can separately evaluate the spectral and diffuse reflectivities of surfaces. A phase locked detection system for the reflectometer is also described. The second item is a selective coating on aluminum potentially useful for flat-plate solar collector applications. The coating is composed of strongly bound copper oxide (divalent) and is formed by an etching process performed on an aluminum alloy with high copper content. Because of this one step fabrication process, fabrication costs are expected to be small. Process parameters, however, need further definition. The third item contains conclusions gleaned from the literature as to the required optical properties of flat plate solar collectors.

Contents

1. Introduction

This is the final report under contract NAS8-32481; The project was directed toward development and understanding of selective surfaces suitable for use in flat plate collectors. The accomplishments of the project are included under the following categories:

1. Development of facilities for parameterization of selective surfaces. In particular a reflectometer has been developed which separately measures the specular and diffuse components of surface reflectivity over the desired spectral range. We believe the reflectometer and method of data analysis to be novel and of possible general utility for reasonably accurate total reflectance measurements with simple equipment. The implementation of a simple phase locked amplifier for detection of small light signals is also discussed.
2. Development of an inexpensive selective coating on aluminum for solar collector use. The surface described here is simply fabricated from the appropriate aluminum alloys and has "good" selective properties. Coating stability is however somewhat spurious although it is believed that further work will solve such problems.
3. Literature investigations to determine properties and preparation methods of selective surfaces and their application to flat plate solar collectors. We were particularly interested in theoretical explanations of selectivity with the view toward optimization of surface parameters through an understanding of selectivity mechanisms. Results of the survey are briefly summarized in this report.
4. Conclusions as to the parameterization of selective surfaces under given applications. In particular the degree of selectivity required for application conditions is discussed.

5. Other lines of investigation pursued by this contract which were not carried to any conclusion.

Most of the work of this contract was accomplished during the first two quarters of the contract period. The main achievements have been the development and partial parameterization of selective surfaces on aluminum by our technique and the development of a reflectometry technique. Recommendations for further work are included in the text.

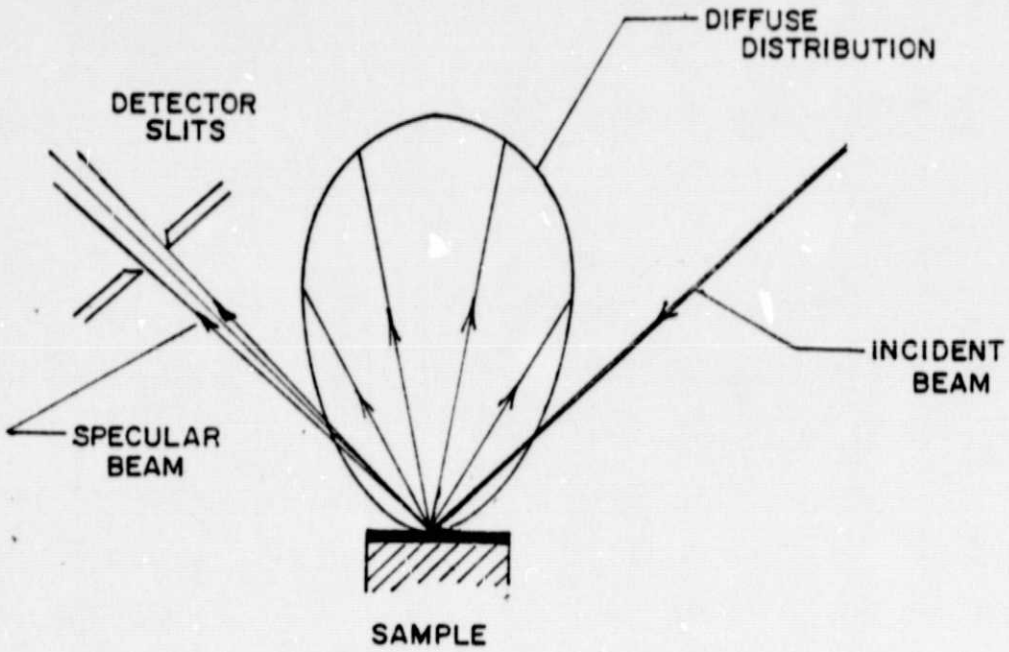

Figure 1: Illustration and definition of the specular and diffuse components of light reflected from a surface. Note that a reflectometer adjusted to measure specular radiation fails to detect most of the diffuse component.

2. Reflectometry of Surfaces With Both Diffuse and Specular Characteristics

2A. Reflectance Measurements

In general, evaluations of selective surfaces found in the literature have been accomplished through specular reflectance measurements. Such measurements are simple to perform and give a quick figure of merit for surfaces which are essentially specular. However, large errors can be made for surfaces which do not exhibit overwhelmingly specular behavior. For example, surfaces have been reported with regular faceting on a microscopic scale which exhibit intense reflection lobes in their angular distributions at angles depending on the inclination and size of facets and direction of incident light. Less exotic surfaces may reflect in part specularly and partially scatter light in a diffuse manner (e.g. a dusty mirror). In general the diffuse reflection from such a surface will have a Lambertian distribution as in Fig. 1, i.e. proportional to the cosine of the angle from the surface normal for light incident near the normal direction. The specular reflection is, of course, located in a narrow angular interval.

From Fig. 1 it can be seen that if a substantial portion of the reflected light lies in the diffuse distribution large errors will be made in the measured reflectance, defined as the ratio of radiation power detected to that incident. This is so since only a small portion of the diffuse light is intercepted by the detector.

2B. Specular and Diffuse Reflectances

In order to parameterize selective surfaces it is necessary to measure the "spectral hemispherical reflectance" for small angles of incidence ϕ from the surface normal. This quantity is defined as

$$\rho(\phi,\lambda) = \frac{\int S_r(\phi,\lambda,\theta,\ell)\ d\Omega}{I_o(\phi,\lambda)} \qquad (1)$$

where λ is the wavelength, θ and ℓ the polar and azimuthal angles about the surface normal, S_r the reflected light intensity per unit solid angle and I_o the total incident light intensity in a narrow beam of negligible angular dispersion. The integral is over the solid angle $d\Omega$ characterized by θ and ℓ and includes the entire hemisphere of reflected light. Here ℓ is referenced from the azimuth of the incident beam.

To a good approximation S_r can be divided up into a diffuse and a spectral part i.e.,

$$S_r = S_s + S_d \tag{2}$$

where S_s takes on appreciable values only for $\ell = \pi$ and $\theta = \phi$. Note that ϕ is a relatively unimportant parameter since only "unusual" surfaces sustain substantial variations in reflectance with angle of incidence less than 60°. In any case solar applications require a small value of ϕ. Dropping the dependence on ϕ and substituting (2) into (1)

$$\rho = \frac{I_s}{I_o} + \frac{\int S_d(\theta,\ell)\, d\Omega}{I_o} \tag{3}$$

where the integration over the spectral distribution has been performed to give the specular intensity, I_s, in a narrow solid angle and where the wavelength parameter, λ, has been omitted as implicit. An explicit form for the diffuse angular distribution of reflected light, $S_d(\theta,\ell)$ is assumed. The form is arbitrary but must nearly coincide with a reference distribution (for later experimental calibration) which for nearly all possible cases of interest will be the Lambertian distribution, i.e. $\alpha \cos\theta$. This will give an explicit value to the second term of Eqn. 3; call it I_d/I_o. Defining the two terms as ρ_s and ρ_d, the spectral and diffuse

Figure 2: A reflectance plot for a diffuse copper oxide surface. Data below 2 microns are total hemispherical while those above are specular

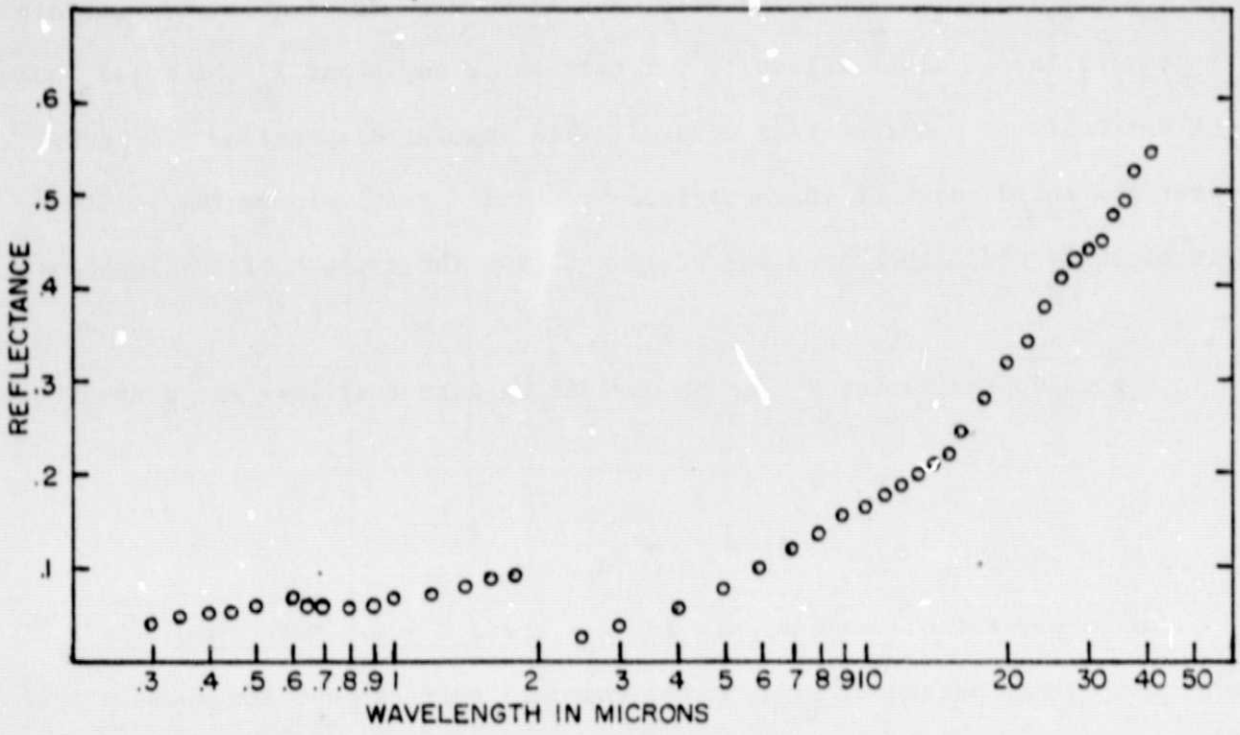

Figure 3: Schematic of a reflectometer for measurement of diffuse and specular reflectances

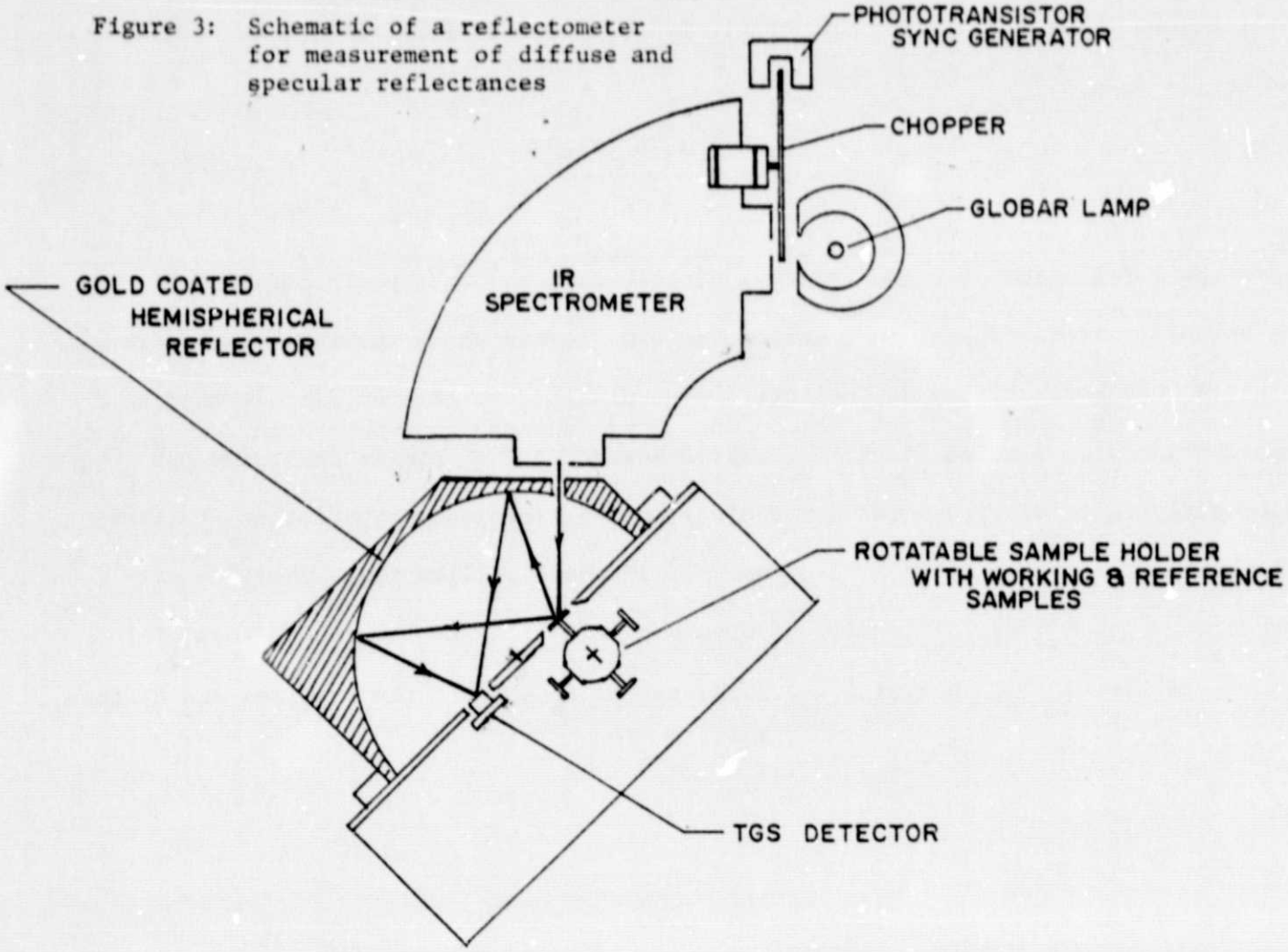

hemispherical reflectivities respectively, Eqn. 3 becomes

$$\rho = \frac{I_s}{I_o} + \frac{I_d}{I_o} = \rho_s + \rho_d \qquad (4)$$

From the above it can be clearly seen that specular reflectometers are in error by the magnitude of the last term in Eqn. 4. We have experienced difficulty in interpreting our measurements and those of others because of the existence of a diffuse reflected component as shown in Fig. 2. A clear example of this occurs in comparing the reflectance of an MgO coated surface with a gold surface. The measured gold reflectivity may be several times that of an MgO coated sample even though the total hemispherical reflectivities are very nearly the same (~0.98 in the near infrared).

Total reflectance measurements can be accomplished most accurately through a diffuse integrating sphere whereby the collection efficiency for reflected light is independent of angle. This method, however, suffers from sensitivity problems and is difficult to extend into the infrared. A supposedly "good" integrating sphere device we had access to failed the gold-MgO test. Unless elaborate precautions are taken, the integrating sphere and other integrating approaches will usually underemphasize the diffusely reflected light.

2C. Reflectometer Geometry

We have developed a procedure whereby a simply constructed, inexpensive reflectometer can be used to assess both spectral and diffuse reflectivities. The reflectometer is shown in Fig. 3 and consists of a suitable light source (tungsten in the visible and a globar in the infrared), a chopper with a phototransistor sync signal generator for later synchronous detection of the light signal and a dispersive instrument, in our case a salt prism spectrometer covering the range from 0.6 to 20 microns. The chopped dispersed beam enters a gold coated hemispherical reflector and is reflected by a sample or reference surface mounted on an indexed

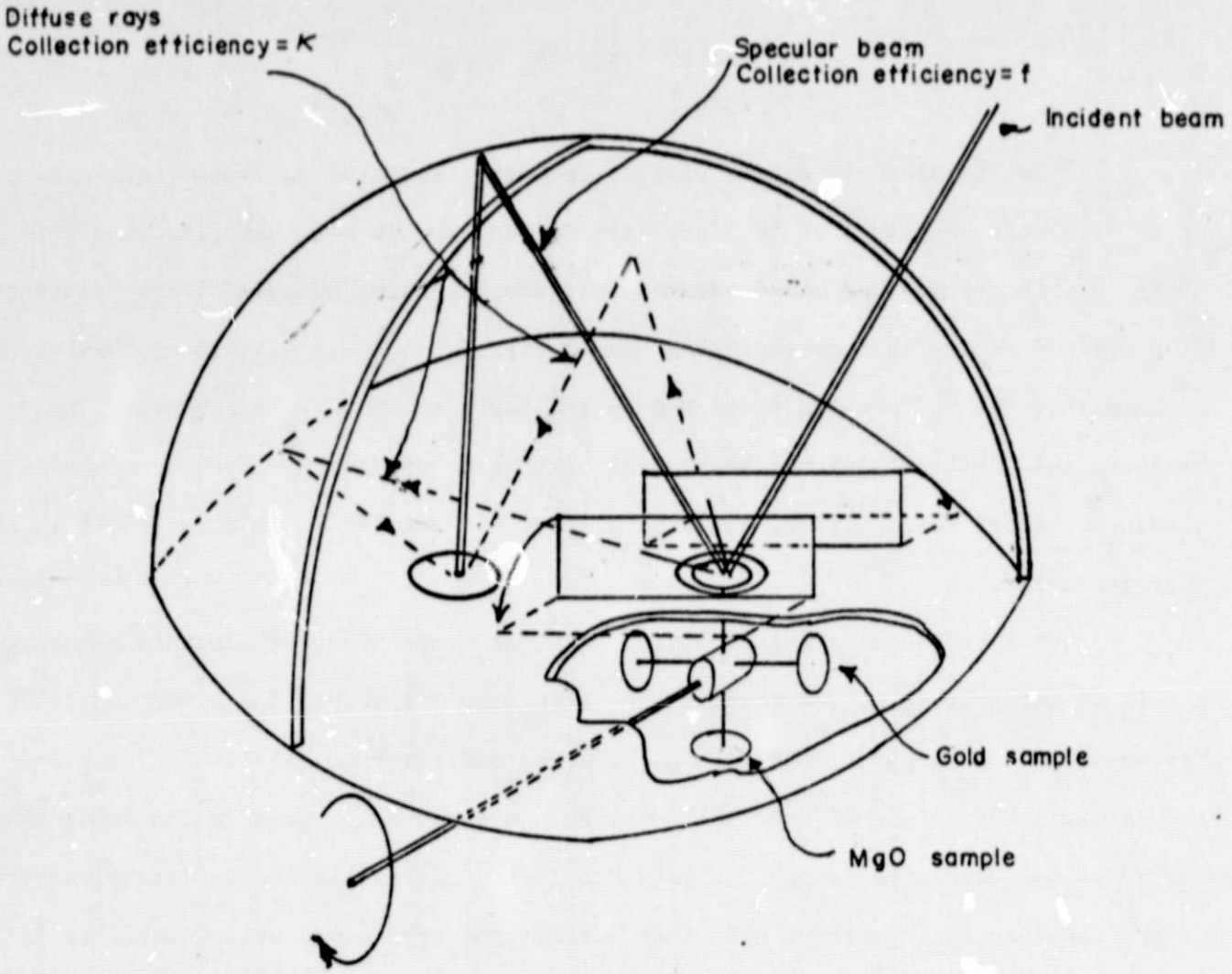

SCHEMATIC OF REFLECTOMETER OPTICS

Figure 4

rotatable holder which accurately positions one of four disc shaped samples at a point off the center of the hemisphere and near a diametral plane. The reflected light is focussed onto a triglycine sulphate detector located at an optically conjugate point. Since the hemispherical mirror is a low order focusing device not all of the reflected light strikes the 1 mm^2 detector. Detector, mirror and sample positions are independently adjustable. Hence, although alignment procedure is clearly defined it is tedious and lengthy.

Reflectometer geometry is shown more adequately for discussion in Fig. 4. In addition to the elements shown in Fig. 3 a pair of light absorbent "flaps" are insertable into the path of the diffusely reflected light without interfering with the specular beam. Flap positioning is non-critical and need only remain constant during a single set of measurements at one wavelength as long as no portion of the specularly reflected beam is intercepted. The sample holder contains two samples under investigation as well as a carefully prepared MgO surface and a glass disc onto which a layer of gold has been evaporated. The reflectometer is adjusted so that: (1) readings for both the gold and MgO samples are independent of which holder the sample is mounted and (2) mirror and detector positioning are such that readings do not depend on small deviations of the sample holder shaft angle about index points.

2D. Data Reduction: Theory

As shown above it is possible to divide the light reflected by a surface into specular and diffuse components. For perfect collection efficiency of both components the light collected R is

$$R = \rho_s I_o + \rho_d I_o \tag{5}$$

For a non-ideal system the measured value of R will be modified by the instrumental collection efficiency. In general this collection efficiency will differ for the

two components with a smaller value for the diffuse light and will depend on reflectance angle and detector and collector geometries. If f is the efficiency of collection for a purely specular sample and assuming a reflectivity of unity for a specular gold surface, the gold intensity will be

$$R_{Au} = fI_o \tag{6}$$

For a high reflectivity with a Lambertian distribution of reflected light, such as MgO, let the collection efficiency be κ. Then the MgO intensity will be

$$R_{MgO} = \kappa I_o \tag{7}$$

For an arbitrary sample the collected light intensity will be approximately given by R_t where

$$R_t = f\rho_s I_o + \kappa\rho_d I_o \tag{8}$$

Eqn. 8 will of course only hold for surfaces with an angular reflectance distribution like that of MgO or whatever reference sample is used. This assumption will be correct for effectively incoherent surfaces but large errors are possible for unusual cases.

From eqn. 8 it can be seen that the two reflectivities are

$$\rho_s = \frac{1}{I_o}\frac{\partial R_t}{\partial f} \quad ; \quad \rho_d = \frac{1}{I_o}\frac{\partial R_t}{\partial \kappa} \tag{9}$$

While many schemes come to mind for the measurement of these derivatives we have chosen to rearrange eqn. 8 by dividing through by eqn 6;

$$\frac{R_t}{R_{Au}} = \rho_s + \frac{\kappa}{f}\rho_d \tag{10}$$

where $\frac{\kappa}{f}$ may be experimentally determined by the ratio of Eqn. 7 to Eqn. 6. A similar relation may be obtained by inserting the flaps in Fig. 4 to block some of the diffuse

component (about 30% blockage is a convenient experimental figure). The new intensity in this case is

$$\frac{R_t'}{R_{Au}} = \rho_s + \frac{\kappa'}{f}\rho_d \tag{11}$$

with κ'/f determinable by Eqn. 3 with the flaps in position, e.g.,

$$R_{MgO}' = \kappa' I_o \tag{12}$$

while, by construction of the flaps R_{Au} remains unchanged.

A reflectivity determination can then be made for a given wavelength by measurement of R_{Au}, R_{MgO}, R_{MgO}', R_s and R_s' and simultaneous solution of equations 6, 7, 10, 11 and 12. This can be done by computer or rapidly by hand since a closed expression for the reflectivities can be found, specifically

$$\rho_d = \frac{R_t - R_t'}{R_{MgO} - R_{MgO}'}$$

$$\rho_s = \frac{R_{MgO}}{R_{MgO} - R_{MgO}'}\,\frac{R_t - R_t'}{R_{Au}} - \frac{R_t}{R_{Au}} \tag{13}$$

The accuracy of the method depends primarily on the accuracy to which R_s and R_s' can be determined; i.e. it can be shown that the relative error in ρ_s and ρ_d is

$$\frac{\Delta\rho_s}{\rho_s} = \frac{\Delta\rho_d}{\rho_d} = \frac{\Delta(R_s - R_s')}{R_s - R_s'}$$

where $\Delta(R - R_s')$ is the uncertainty in the measurement of these two quantities. If the collection efficiency is not adequate it is possible that $\Delta(R_s - R_s')$ may be limited by instrumental sensitivity. We have encountered this problem in our instrumentation at the wavelength extremes of light sources due to the fact that our detector

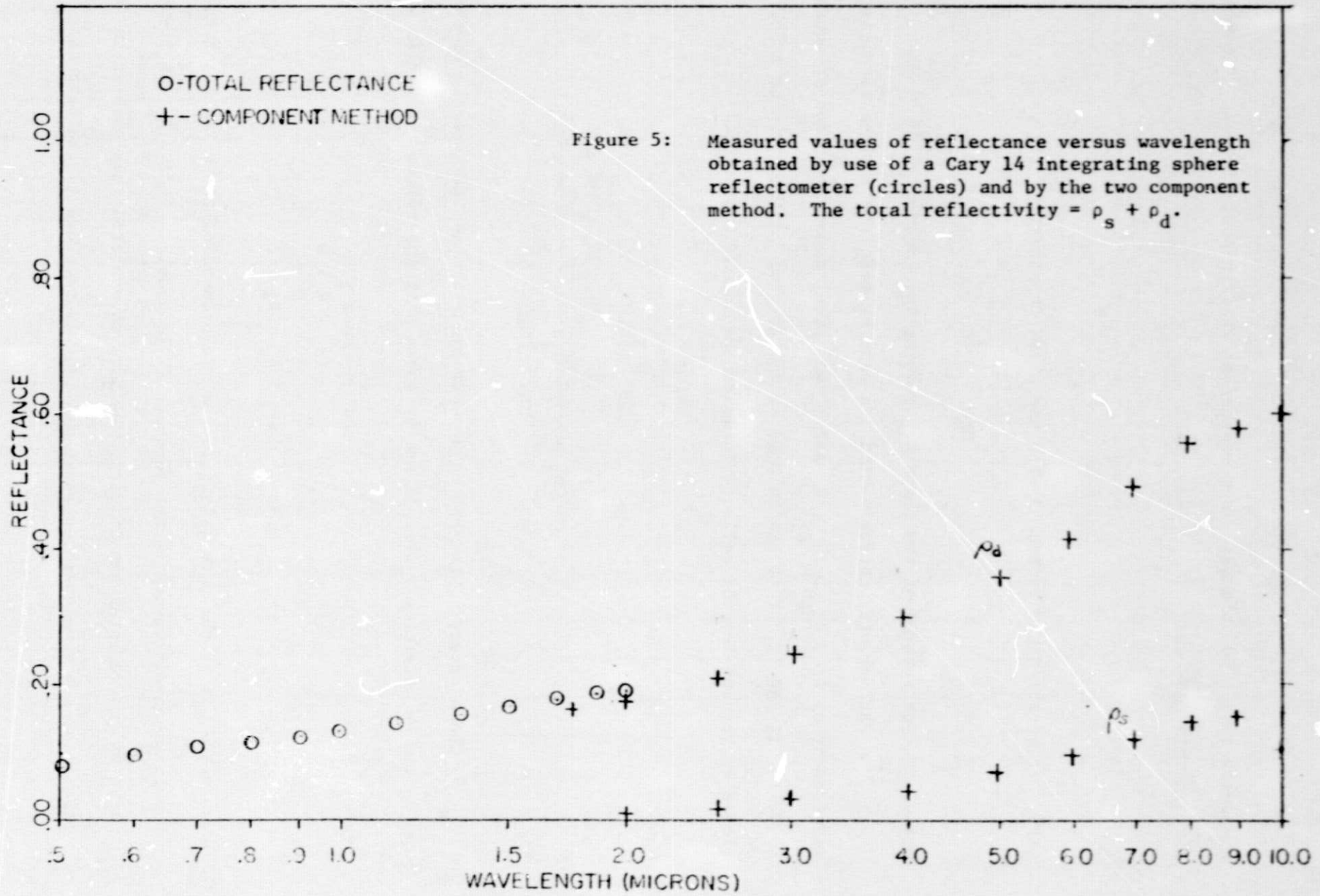

Figure 5: Measured values of reflectance versus wavelength obtained by use of a Cary 14 integrating sphere reflectometer (circles) and by the two component method. The total reflectivity = $\rho_s + \rho_d$.

area is small (1 mm^2) and hence a small value of κ/f is obtained because of the width of the diffuse image at the detector. A "perfect" focusing system (e.g., an ellipsoidal collector mirror) or a larger detector should eliminate this problem.

More rapid approaches to gathering data than the above procedure could involve chopping of the diffusely reflected light with direct readout of the two reflectivities through a small analog or digital computer. Other changes which would increase the general utility and speed of the device can be envisioned.

A reflectance curve obtained with this apparatus for a primarily diffuse surface is shown in Fig. 5.

2E. Reflectometer Electronics

In line with our small equipment budget we have designed a simple amplifier for detection of the small light signals involved in the reflectometer implementation. Figure 6a illustrates the mechanical layout of the light detection system. Light from the source is chopped at a frequency of 107 hertz by a three-bladed mechanical chopper driven by a synchronous motor. The chopper also interrupts a beam from a D.C. driven light emitting diode producing a square wave reference signal as output of a phototransistor. This reference signal is mechanically adjusted to be in phase with the signal beam and after amplification (by a 741 OpAmp-not shown) is fed to the reference signal input in Fig. 6b.

The chopped light signal is dispersed by the monochromator, analyzed by the reflectometer and detected by a triglycine sulphate detector. A change of impedance to about 10K is effected by a FET preamp located within the detector casing. The signal is then capacitively coupled to a two stage amplifier using 536 FET operational amplifiers. The amplifer has gain variable from 300 to 10,000. The emergent signal is buried in 60 hertz noise and a gray background. It then passes through a demodulation circuit driven by the reference signal. During the low phase

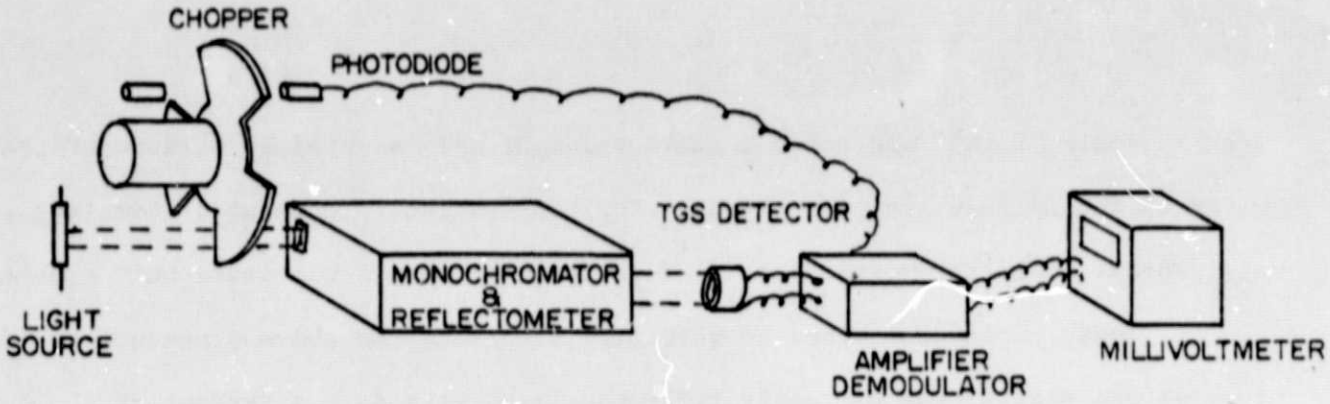

Figure 6a

IMPLEMENTATION OF SYNCHRONOUS
LIGHT DETECTOR (SCHEMATIC)

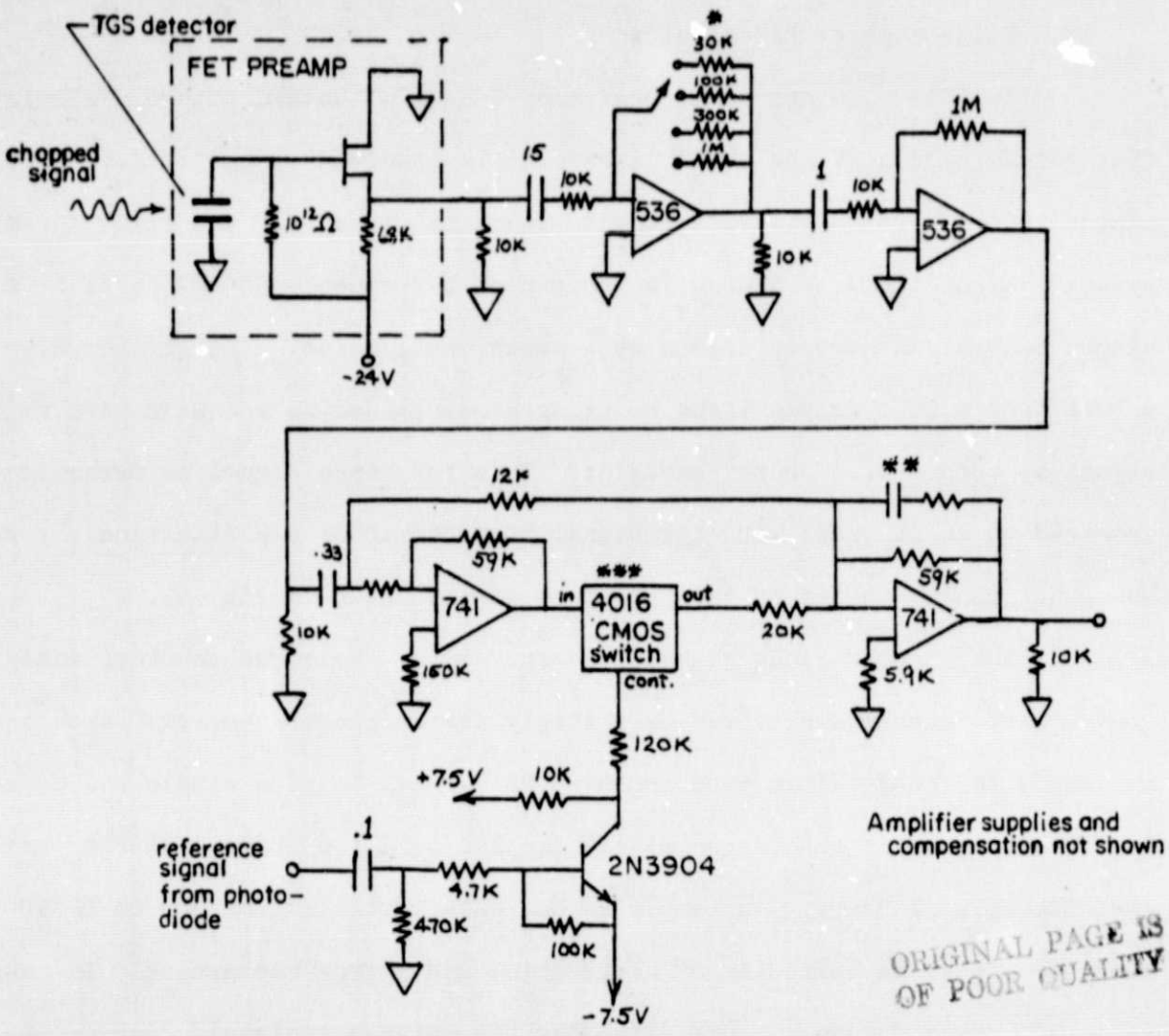

Figure 6b

* filter capacitor across feedback resistors to prevent high frequency oscillation

** capacitor with small damping resistor controls low frequency noise

*** CMOS switch powered by ±7.5 V.

SYNCHRONOUS AMPLIFIER CIRCUIT SCHEMATIC

of the reference signal the CMOS switch is off and the 12K resistor acts as the input resistor for the second 741 operational amplifier in Fig. 6b. With a 59K feedback resistor the net demodulator gain is -5. During the positive phase of the reference signal the CMOS switch conducts so that both amplifiers are operative. The feedback resistors are arranged so that the gain is now +5. If the detector signal is in phase with the reference signal there is a net D.C. voltage on the demodulator output proportional to the signal. For frequencies other than the chopping frequency the phase relative to the chopper phase will vary rapidly with time producing no net D.C. output. It is advantageous to increase the output amplifier time constant by means of an RC filter in parallel with the feedback resistor. This eliminates low frequency output fluctuations.

The amplifier is capable of detecting signals of less than 0.1 microvolt from the preamp output corresponding to a light intensity detection threshold of about 3×10^{-10} watts/mm^2. The amplifier band pass is not directly measureable but an active filter with a 1Hz. bandpass placed on the detector input produces no change in the noise or signal intensity. Behavior with smaller bandpass filters was difficult to assess since the chopper frequency drifted in and out of the fixed bandpass region. A very narrow bandpass filter could possibly increase noise rejection. However narrow bandwidths require either filter tracking or close chopper frequency control. Sixty hertz rejection was such that the unshielded apparatus could be used with the fluorescent room lights on even though this resulted in a fivefold increase of noise to the demodulator input.

3. A Selective Absorbing Copper Oxide Surface

3A. Surface Selectivity

Addition of selective properties to absorbing and transmitting surfaces of solar collectors improve collector efficiency by preventing reradiation of absorbed energy. The ideal transition wavelength of an absorber from low to high reflectance depends on collector temperature but for most applications there is little overlap between the solar spectrum and the reradiation distribution. A nominal figure for the transition wavelength lies between 2 to 4 microns. The degree of selectivity required or desireable for maximum efficiency depends on the collector temperature and other application parameters. Some of the practical aspects of selectivity requirements are discussed in section 5 of this report and literature references to basic concepts of selectivity are there given along with the references contained in section 4. We have used the reflectance $\rho(\lambda)$, at wavelength λ, for the parameter characterizing selective properties. Other discussions use the emittance $\varepsilon(\lambda)$ or the absorptance $\alpha(\lambda)$ as parameters characterzing the surface. The relationship between these parameters is simple. Assuming that there are no unusual channels for conversion of radiation to other wavelengths (e.g., fluorescence) energy conservation for an opaque material requires that

$$\rho(\lambda) = 1 - \alpha(\lambda)$$

and that

$$\varepsilon(\lambda) = \alpha(\lambda) \quad .$$

Selective materials are usually evaluated as to quality by the size of the selectivity parameter α/ε where α is the average absorbtance at visible wavelengths and ε is the average infrared emittance. A "good" value for the selectivity parameter is around twenty with α greater than 0.95 and ε less than 0.5. As we note in section

4 extreme care must be exercised in this figure of merit. Trade-offs between α and ε to achieve high selectivity may decrease collector efficiency as well as cost effectiveness.

The theoretical basis of selectivity is not well founded. In general the phenomenon involves three factors which in most cases combine to form the surface properties:

(1) The material electronic band structure as modified by size effects. Most selective materials have band structure such that an absorption edge in the bulk material occurs not "too far" from the selective transition wavelength. The absorption edge and selective wavelength however are apparently not simply related for thin layers or powders.

(2) Particle size effects. It is well known that surface geometry affects reflectivity. In particular a surface with an abundance of small deep pits will absorb light at short wavelengths. However, as the ratio of mean square surface roughness to wavelength decreases far below unity, surface reflectivity increases. This is a presumed mechanism for the selective properties of gold black. Particle size effects may also be expected to affect material optical properties.

(3) Interference effects. A thin dielectric layer on a reflective surface is well known to cause interference effects. Multiple layer coatings have been used to fabricate selective surfaces.

It is likely that all three of these effects combine to some extent to produce observed selectivity.

Many types of coatings using both inorganic and organic materials have been developed which exhibit selective properties. The coatings with organic components (In general paints) have been expensive and often unstable with respect to

infrared reflectance. Inorganic coatings show greater stability and can often be tailored to desirable reflectance curves, but are in general expensive to fabricate and may require exotic substrates. A noteable exception to this has been black chrome coatings which have achieved commercial viability and appear to be very durable. To date, however, we know of no process for fabricating black chrome coatings on aluminum. Copper is used for the substrate and recently techniques have been developed for laminating thin sheets of coated copper to aluminum bases. A more desirable process would directly utilize on aluminum substrate, have an inorganic coating, and be inexpensive to fabricate.

Our approach to the development of a surface meeting these criteria utilizes material present in the substrate as a component of the selective coating. Specifically we have chosen aluminum alloys with high copper content. By chemical etching of the aluminum a matrix of copper oxide is left on the surface. Alloys with high nickel content produce nickel oxide coatings which is of interest since nickel oxide coatings are known to be selective. However, nickel aluminum alloys are not suitable for solar collectors because of poor malleability and high cost.

3B. Formation of Impurity Oxides on Etched Surfaces

The formation of "smut" on alloy surfaces during cleaning and electrolysis operations has long been a bane to processing operations. The smut forms in general, due to residual alloy constituent oxides which are not soluble in the chemical bath. Experience with cleaning aluminum alloys by etching in strong bases led us to believe that coatings of selective materials might be formed during such processing. It is well known that thin films of nickel or copper on highly reflective substrates can produce selective coatings.

The mechanism for impurity oxide formation has not to our knowledge, been elucidated and in itself forms an interesting field for possible study. We have

found that, for many of the cases investigated by us, the oxide layer forms an interlaced matrix of small granules spaced at approximately the metal grain size with relatively strong cohesion and substrate adhesion. In other cases the layer is microscopically coherent so that interference colors are visible. The granular case which occurs with annealed alloys may involve either initial impurity aggregation around metal grain boundaries, intergranular solution precipitation, or oxide crystallization about the disappearing grain as it dissolves in the etchant. The coherent case occurs with tempered alloys and results in a continuous coating indicating uniform impurity dispersion. These results may either reveal interesting facts about the spatial distribution of material in an alloy or describe surface etching on a microscopic scale. We did not investigate the mechanisms of oxide formation except as related to optimization of surface selectivity. However, unless explanations for the phenomena we observed lie in the scattered literature of surface chemistry, further work is appropriate and may have applications to surface treatment procedures and corrosion control.

3C. Incoherent Coatings

Alloys with low copper content such as 2024 (4.5%) upon etching in sodium hydroxide or other suitable strong base produced weakly bound powder-like coatings with mildly selective properties. Increasing the copper content to 6.3% by using 2219-0 samples produced a blacker surface with better cohesive and optical properties. A plot of reflectance versus wavelength for a heavily coated surface produced by etching of sand blasted 2219-0 aluminum in 2N NaOH for 10 minutes is given in Fig. 5. The coating is mainly diffuse.

The chemical composition of the coating was confirmed by x-ray fluorescence spectra to be the predominant heavy element (i.e., atomic number less than 20) and its oxidation state infered from color and relative solubility in nitric acid and

ammonium hydroxide. Optical and scanning electron microscopy indicate an interleaved matrix of granules and fibers deposited in some manner by the etching process. As previously stated the formation process is probably very interesting. Coating morphology studies of heat treated substrates indicated a correlation between substrate grain size and coating particle dimensions. If the particle size could be tailored to somewhat less than the desired cutoff wavelength, the theory of scattering from powders indicates that the coating would be transparent to long wavelength light (with reflectivity characterized by the metallic substrate) but absorbent for short wavelengths. We were hence induced to study heat treated materials with very smooth surfaces.

3D. Coherent Coatings on Polished 2219-T87 Aluminum

Because of commercial availability we investigated the properties of T87 tempered 2219 aluminum which had been polished by acid bright dipping. We discovered a qualitatively different type of coating which exhibited sufficient coherence to produce uniform interference coloration. After some aging or low temperature baking (50°C) the coatings are comparable to selective paints we have encountered in hardness and durability. Our initial results indicated good high temperature stability with 450°C temperatures for several days, producing little effect upon the coating. However, as discussed later, we have found spurious instabilities after high temperature processing.

Ellipsometric measurements at 0.63 microns show that for thin coatings the growth rate in 1N NaOH is 1100 Å/minute for 2219-T87 aluminum at 20°C. Under these conditions the freshly prepared coatings have a real index of refraction, n, of 1.05. The imaginary part of the index of refraction, k, often called the attenuation coefficient, was 0.1. Upon baking at 450°C for 24 hours the measurements indicated a rise in n to 1.25, a decrease in k to 0.046 and a 20% decrease in coating thickness, presumably representing a compacting of the coating. The coatings

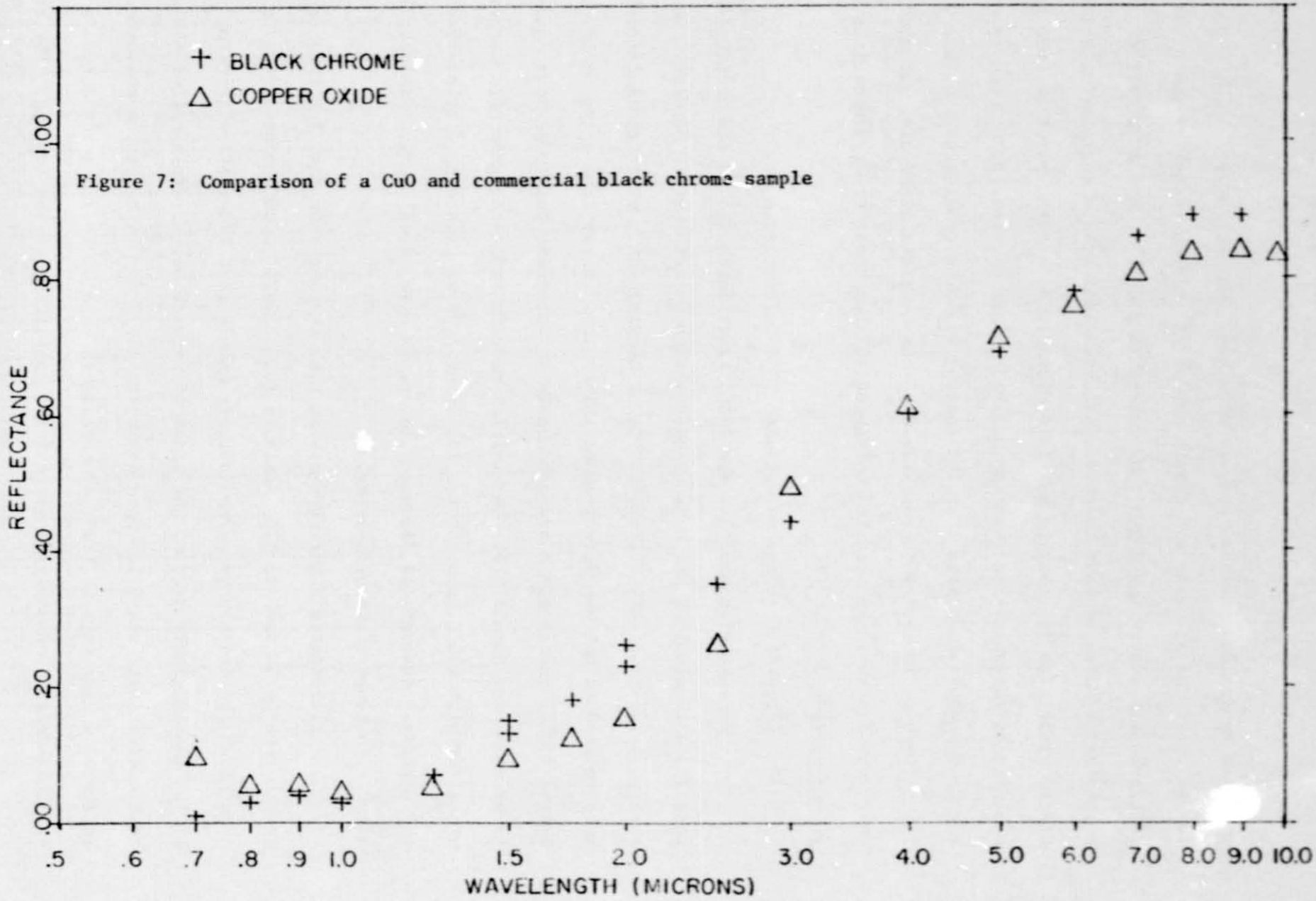

Figure 7: Comparison of a CuO and commercial black chrome sample

produced in 1N NaOH showed rather pale interference colors which changed slightly during the first hour of baking. Futher baking for up to three days caused no perceptible change in coating properties.

Treatment of 2219-T samples in 2N NaOH solutions gave deeper interference colors. We are hence led to believe that the absorptivity (i.e., k) is affected by solution normality. Baking at 450°C produced a shift in color during the first few hours with no further change over several days. In general the samples were bright-dipped to a fair degree of specularity. Rougher samples (e.g. sandblasted surfaces) produced grayer and presumably less coherent coatings. This is possibly due to uneven film formation so that film interference is averaged out over macroscopic surface areas with subsequent enhancement of absorption by small particle scattering.

Coating colors in 2N NaOH evolved to light straw at 1 minute, light blue at 2 minutes, yellow-green at 3, violet at 4, deep green at 5, deep violet at 6, dark green at 7, very dark purple at 8, with successive interference orders appearing at longer times. These times are approximate and will vary with solution properties, surface pretreatment and temperature of formation. Film darkness increased with etching time until after about 12 minutes the interference colors could no longer be observed. An 18-minute sample was extremely black; measurements at 0.8 microns gave a reflectivity below our threshold (about 1%) for meaningful determinations.

Figure 7 shows a plot of reflectivity versus wavelength for a commercial black chrome sample and one of our CuO samples. We are able to obtain much the same optical properties as the black chrome in the infrared. The visible portion of the spectrum was not explored in this investigation but the greenish appearance

of the sample leads us to expect a higher absorbtivity than black chrome in the visible region. In Fig. 7 the aluminum sample was highly polished before etching.

Figures 8 through 15 show some of the curves obtained for a series of unbaked samples for various treatment times. This data is here presented without extensive comment. The samples were bright dipped so that the surface was fairly specular ($\rho_s \sim 0.8$) although for the small sample size used substrate polish was difficult to control. Coating specularity was determined primarily by initial sample specularity and the long wavelength limit for lightly coated samples showed a reflectivity equal to or better than that of the untreated aluminum sample. The samples with lower initial polish showed a higher diffuse component of reflectivity. Data in Figs. 8-15 are uncorrected for diffuse reflectivity and represent the specular reflectivity with approximately 20% of the diffuse component added in. Data were reduced through simply dividing the reflected intensity by that for an evaporated gold sample. Taking this factor into account and incorporating other possible errors, we estimate that correction factors in the data would increase the given total reflectance values by up to 25%. Hence nominal long-wavelength limits for the reflectivities are of the order of 0.9, i.e. approximately the reflectivity of the bare aluminum.

Fig. 8 shows a reflectivity curve for an uncoated aluminum sample which had been bright dipped. The variation in reflectivity with wavelength is believed due to a thin coating of copper oxide (~ 100 Å) left on the surface. Fig. 9 shows the results for a 2 minute sample which appeared light blue; the reflectivity appears to swing upward in the visible region of the spectrum. Figs. 10 and 11 show a bright yellow-green sample (3 min.) and a green-violet sample (5 min.), respectively. Both of these samples show selectivity but are obviously reflective in regions of the visible. Fig. 12 shows data for a sample (6 min.) we believe to possess excellent selective properties; the sample looks extremely black, by actual measurement

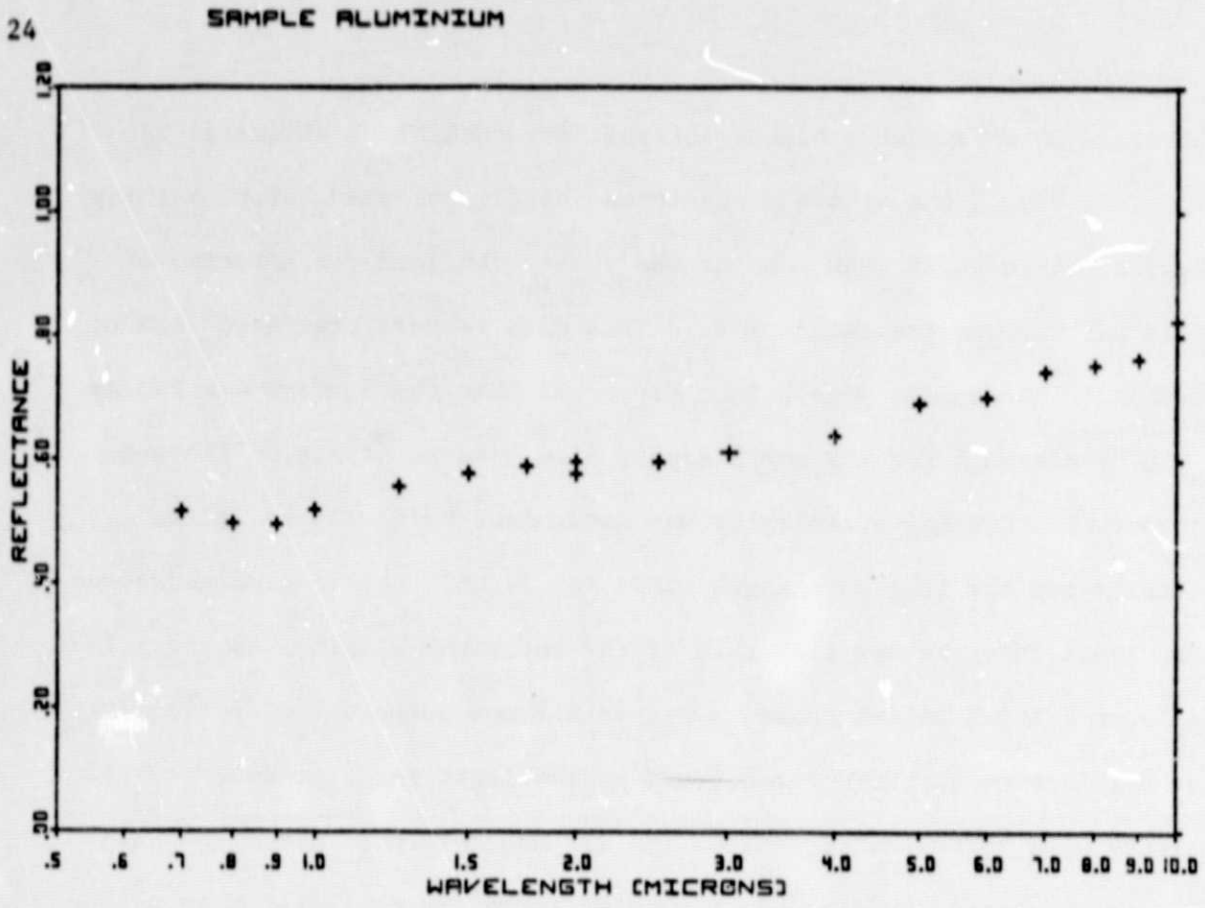

Figure 8

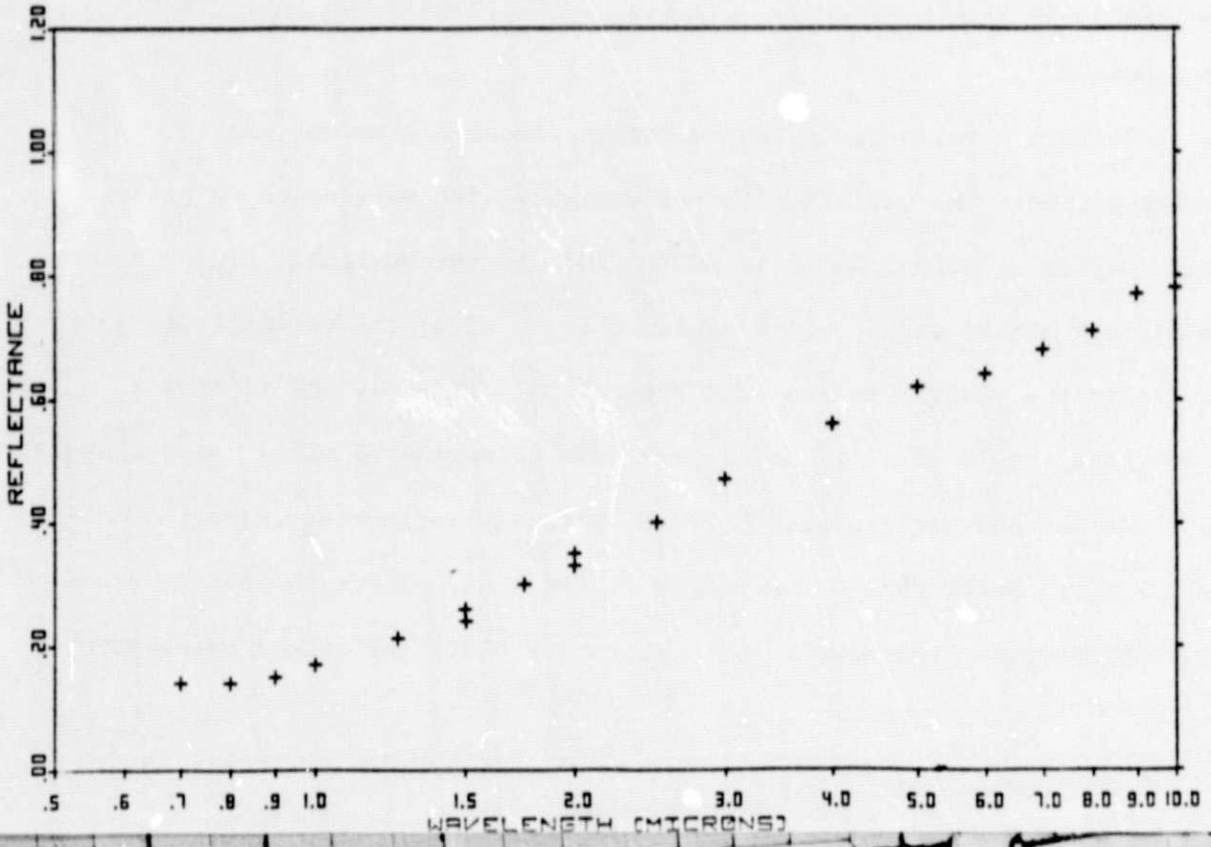

Figure 9

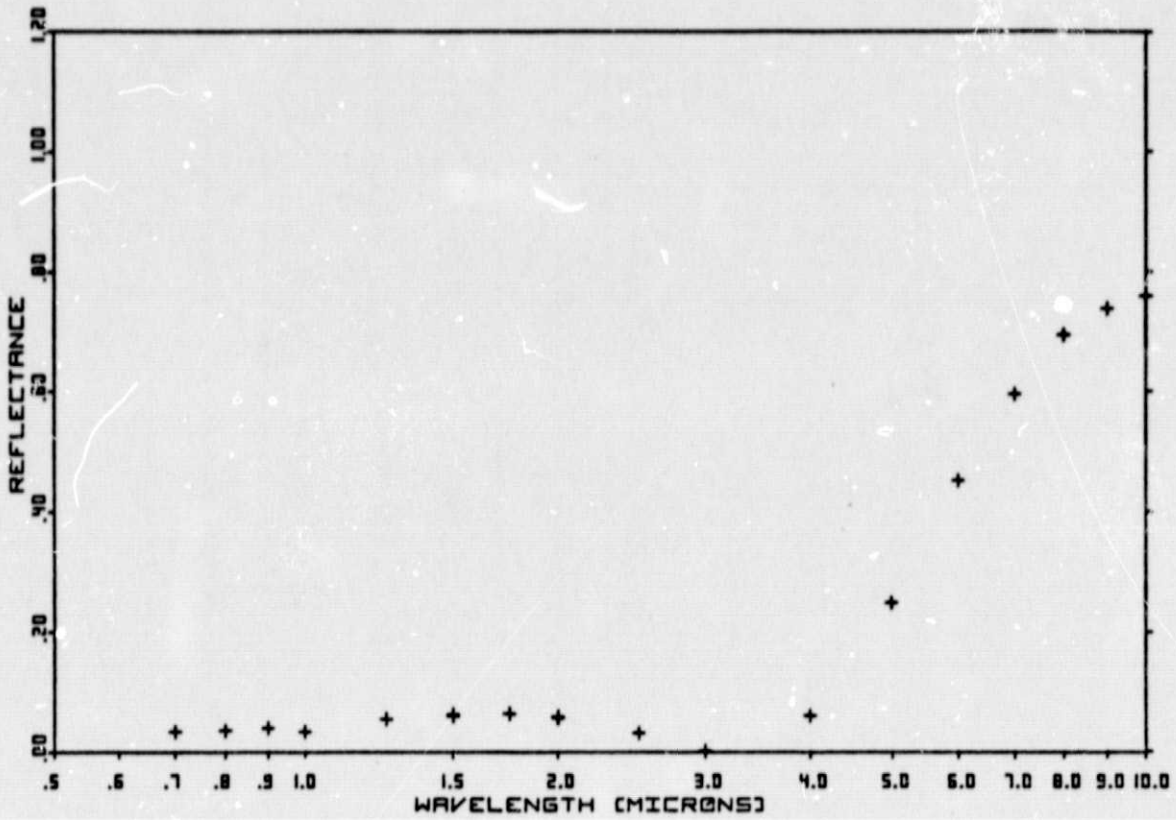

Figure 10

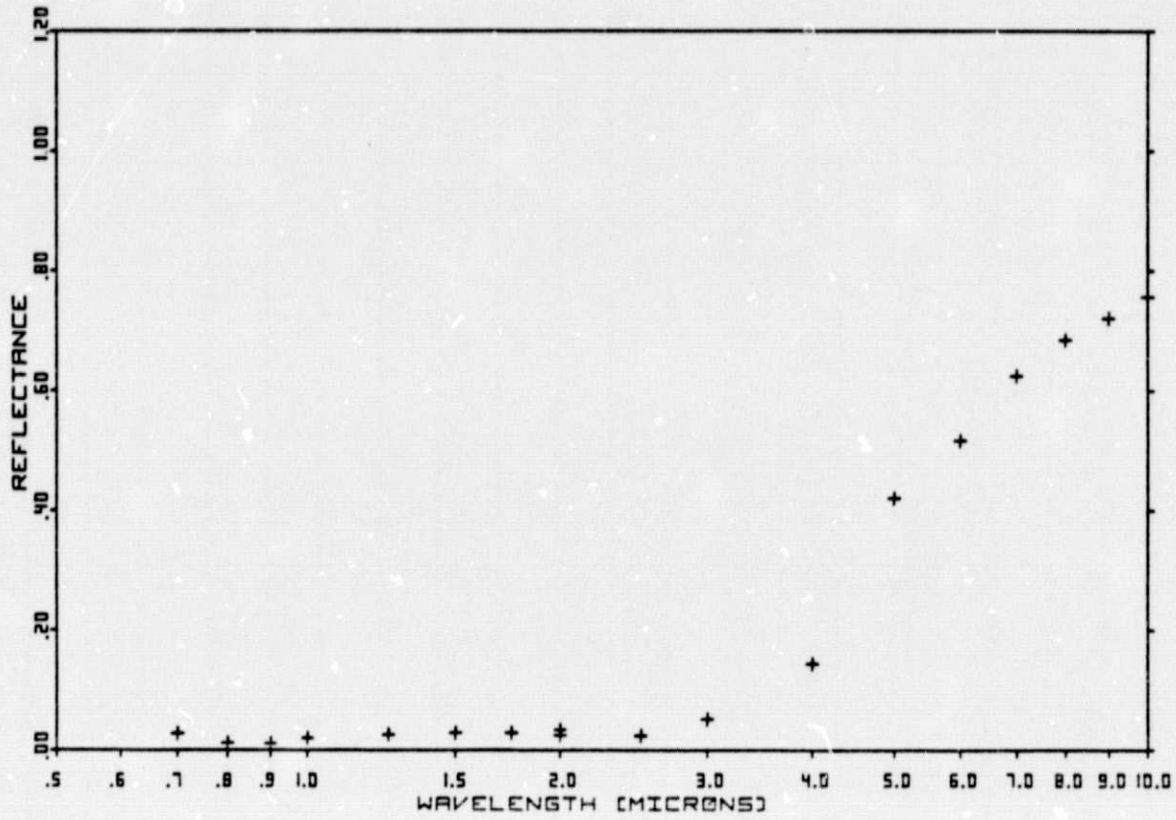

Figure 11

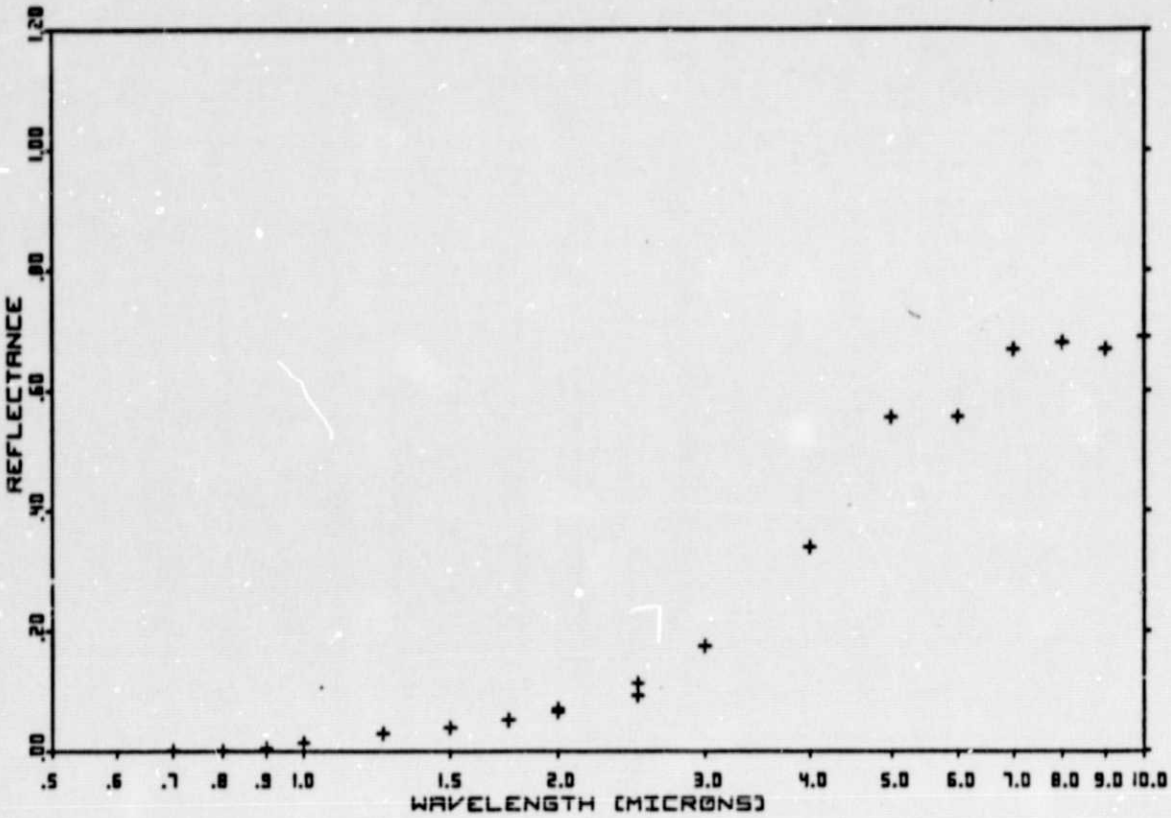

Figure 12

SAMPLE 10

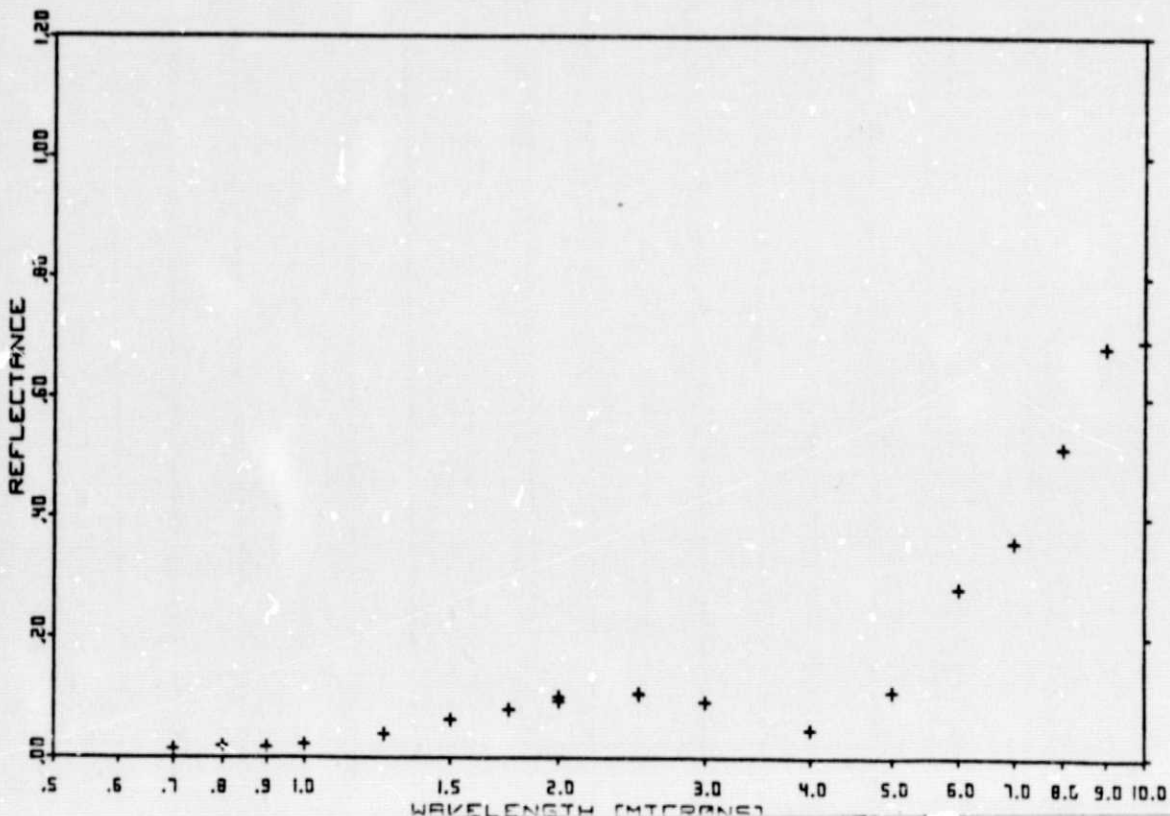

Figure 13

SAMPLE 13

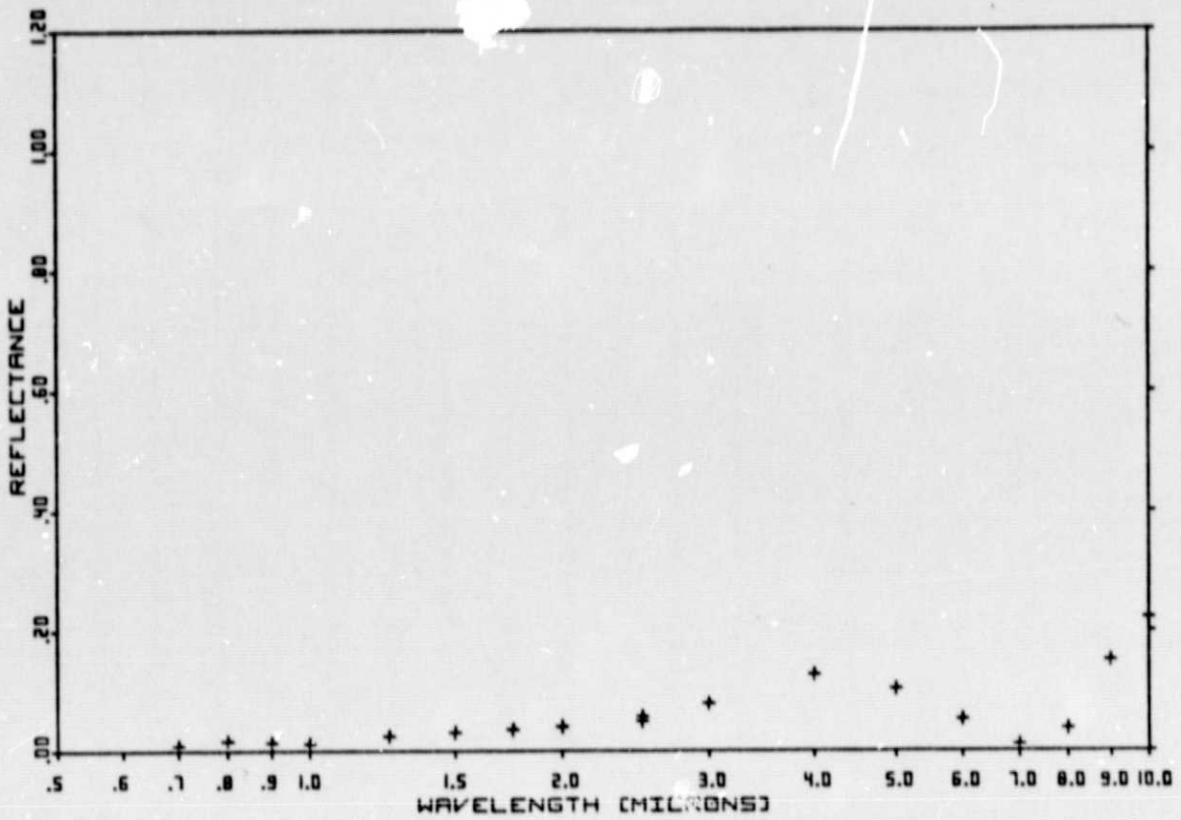

Figure 14

SAMPLE 16

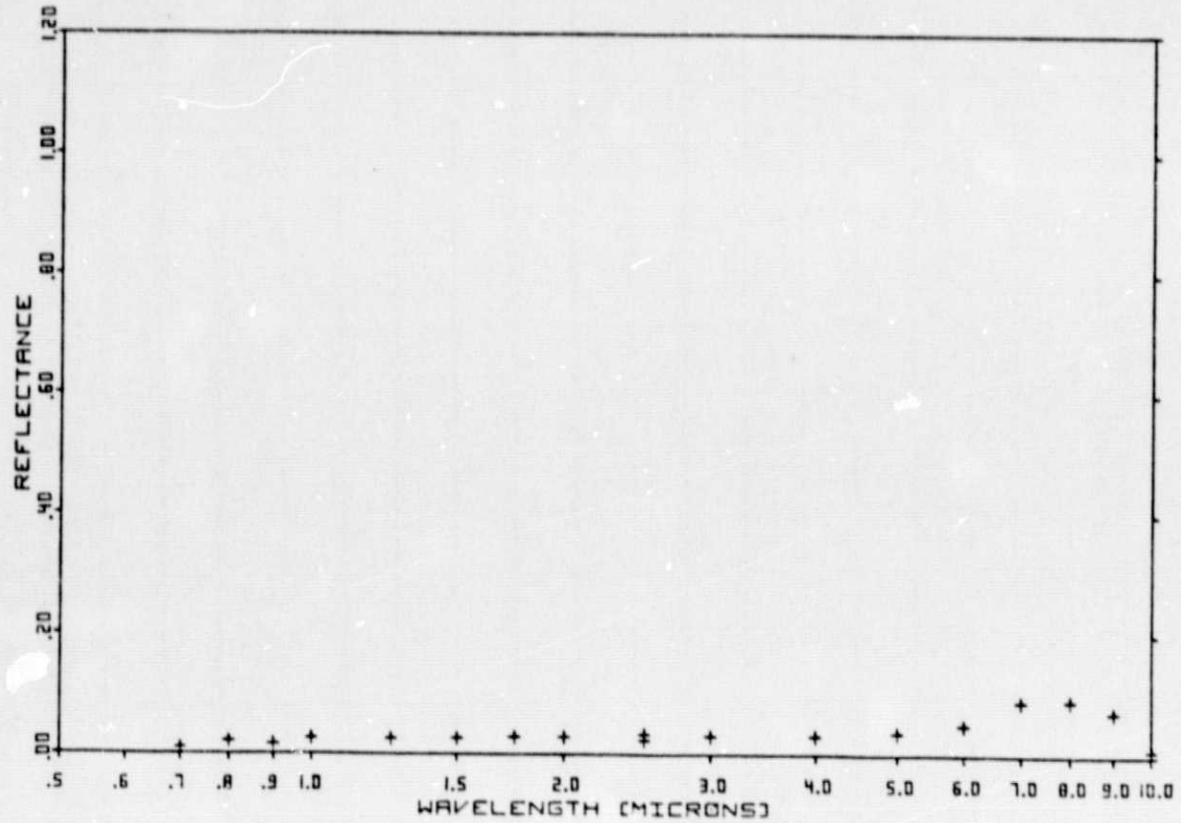

Figure 15

has low reflectivity (< 1%) in the near infrared and high reflectivity (after corrections for diffuse reflections ~ 85-90%) at long wavelengths. Figures 13, 14, and 15 show data for samples treated for 8, 11, and 18 minutes respectively. A general blackening is observed with treatment time with the rise in reflectivity moving toward longer wavelength. The "humps" in the data are believed to be due to interference effects in the coating.

3E. Fabrication and Environmental Parameters

We have spent some time in confirming and investigating the reproducibility of the data presented in section D. We find that the optical properties presented in section D are very reproducible for a given solution normality and alloy composition. However, heat treatment of the coated material does not in every case lead to the same qualitative effects. We believe this spuriousness to be due to coating sensitivity to fabrication parameters. The effects of the parameters heat treatment, substrate surface finish, solution characteristics, alloy composition, and humidity are discussed below.

3E-1. Coating Heat Treatment

Our original experience with heavy coatings led us to believe that the copper oxide coatings were very stable with respect to high temperatures. Many of our samples could be baked out for days at temperatures greater than 400°C with no apparent effect except for an increase in coating cohesiveness and slight color changes. In fact, a corner of a sample could be heated with a torch almost until melting of the aluminum occured with little change in the coating. Light coatings did show appreciable color changes upon baking but this was not felt a disadvantage since the changes were small as discussed in section 3D and could be compensated for by increasing the treatment time. However, more recent results produced spurious

runs in the sense that heat treatment made drastic changes in the coating to the extent of nearly complete coatings disappearance for lightly coated samples. After many experiments we were led to consider the possibility that these changes were due to an interaction of water and residual NaOH on the surface. The evidence for this included the fact that the critical temperature for coating changes occurred at 100°C. The degree of rinsing, a difficult parameter to establish, had an effect on results. We also noted that immersion in boiling water would renew the etching process, indicating residual sodium hydroxide. A further factor also emerged; aging of the samples in air at room temperature for several days increased surface stability against both abrasion and heat deterioration. This fact provides an alternative explanation to the heat degradation phenomenon. Formation of $CuAl_2$ intergranular precipitate occurs at 100°C, possibly causing reduction of the surface coating into the intergranular precipitate. Aging may help prevent this through passive layer formation.

Our observations as to the heat deterioration problem are unfortunately still very qualitative. We note however that with careful control of sample processing, reproducible and small changes occur during heat treatment representing mainly a compacting of the coating. Very heavy coatings, which have not been carefully processed, upon baking provide a hard stable brownish surface with moderate selectivity ($\alpha \sim 0.93$, $\varepsilon \sim 0.3$). These latter coatings may be of some interest. We cannot at this point give an optimum procedure for surface preparation but are convinced that one exists and is worth pursuing. The behavior of the material under thermal cycling is of course a very crucial point for applications.

3E-2. Substrate Surface Finish

Experimental results, demonstrate that initial surface finish is an important factor in coating characteristics. Initially rough surfaces such as produced by sandblasting result in loose granular surfaces which reflect diffusely and

do not demonstrate high selectivity.

Surfaces with smooch mill finishes (presumably highly passivated) and no pretreatment except for degreasing result in fine grained poorly adhering coatings. The best pretreatment for producing coherent coatings that we have used is an acid bright dip to produce a smooth specular surface. The reasons for surface pretreatment dependence are not obvious although speculations as to the effect of original passive layer thickness are possible. An assessment of the amount of material removal needs to be made.

3E-3. Solution Characteristics

Most of our experiments have been done with 2N NaOH as the etchant solution. In accordance with well known corrosion data, the rate of etching increases rapidly with solution pH above 14 which is the nominal pH of a 1N NaOH solution. The coating growth rate, however, decreases with thickness so that like many corrosion processes there appears to be a limiting effect on the depth of the corrosion layer. Solution temperature also has an effect on the coating characteristics. High temperatures (near 100°C) tend to produce very fine dendrite structures which cause the surface to look velvety and very black. We have not investigated the effects of solution temperature except for some qualitative observations. It is likely that solution additions will alter the process significantly. For example it is well known that addition of Cl^- ions strongly affect aluminum corrosion.

3E-4. Alloy Composition

Alloy composition has been discussed previously. A continuous spectrum of copper composition cannot be readily obtained. We have, however, noted that low copper content alloys (< 1%) produce no coating; the copper oxide formed is apparently not dense enough to cohere. Medium copper content (~4%) alloys produce grayer and more powdery coatings than does 2219. Alloy temper has a strong effect on coating characteristics as we have noted above. This too may be related to intergranular

Figure 16: Theoretical curves for reflectance of a coating on aluminum versus coating thickness divided by wavelength. Curve 1 corresponds to a coating with the real and imaginary indices of refraction (n and k) as measured for a fresh thin coating while curve 2 uses n and k as measured for a coating baked for 24 hrs at 400°C.

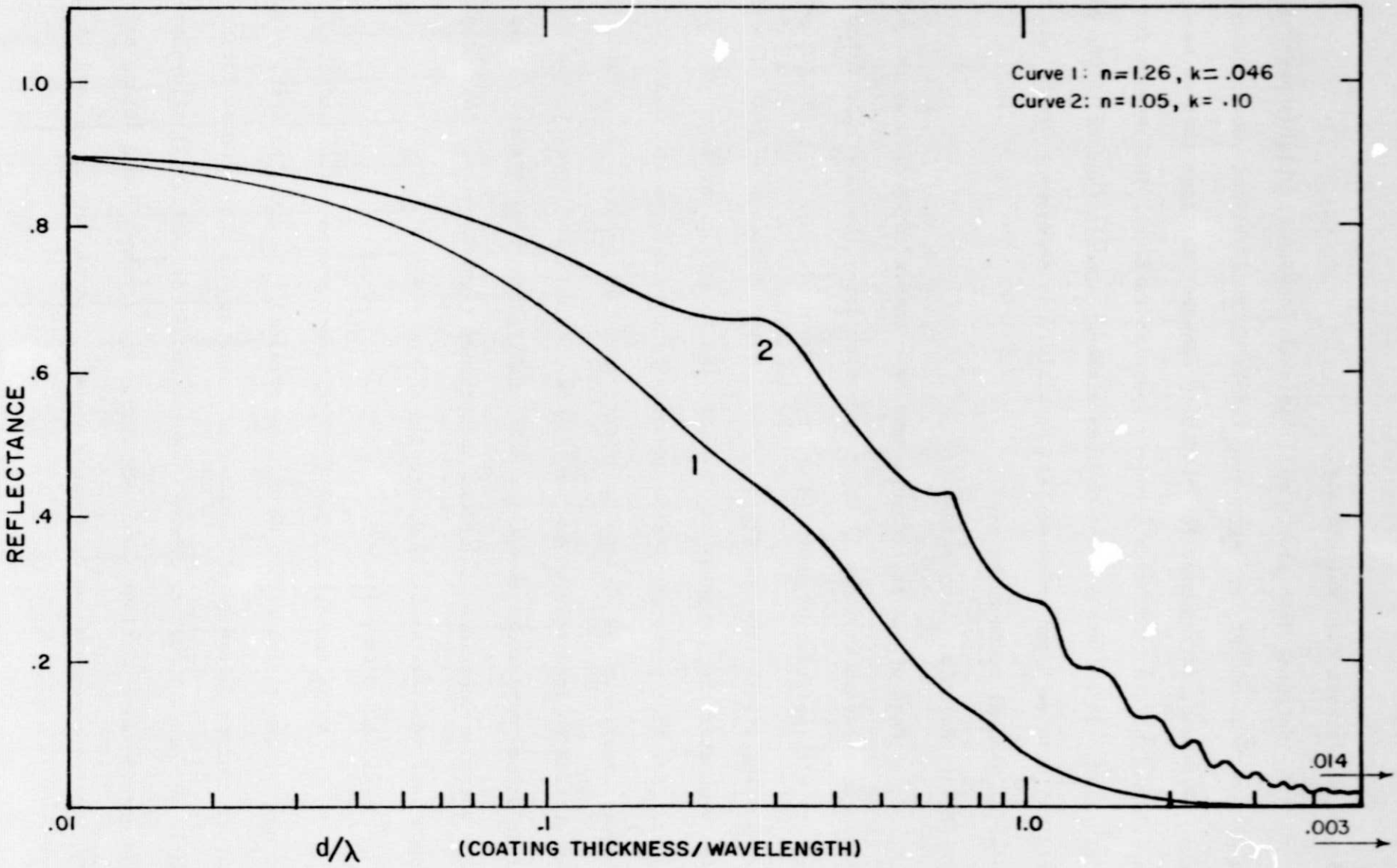

copper precipitation or simply grain size. We have found that high nickel alloys also produce a deep black coating but did not investigate these alloys since they could not be obtained in wrought forms.

3E-5. Humidity

We approximated MIL test specifications for humidity and found little effect on coatings that were well rinsed and aged. Coatings with residual NaOH will resume dendritic growth at high vapor temperatures. Humidity tests are of course important for simulation of applied situations.

3F. Theoretical Investigation of Surface Optical Properties

We consider the coating optical properties to be due to a combination of effects involving particle size, band structure and interference. The effect of particle size is very difficult to evaluate and has not been accomplished except for very idealized and particularized cases. We did not, at any rate, feel that particle size was the predominant consideration for many of the surfaces investigated. Thin coherent coatings are possibly selective due to interference with layer indices of refraction determined by band structure (e.g. multilayer selective surfaces[1]). Using the measured indices of refraction in section 3D along with handbook figures for aluminum and inserting them into the Rayleigh coefficients[2] gives values for the reflectance results in the plot of Fig. 16. The quantitative aspects of the measured curves are not reproduced by this calculation. This might be expected since the indices of refraction presumably vary with wavelength in this region of the spectrum and surface microstructure may be important. We have not completed our work on introduction of the CuO band structure into the calculation.

3G. Summary and Conclusions

The copper oxide surface developed appears to be of possible practical interest for use in flat plate solar collector systems. Light coherent coatings on

2219-T87 aluminum have high selectivity but stability with respect to temperature cycling is not yet reproducible. Heavy coatings which have been well baked have moderate selectivity and will withstand high temperatures. The nature of the coating formation is poorly understood but is believed due to a combination of original $CuAl_2$ intergranular precipitate and process precipitation from the binary solution. Further work is needed on understanding the coating formation mechanism and the optical properties as well as defining procedures to produce durable surfaces.

4. Summary of Literature Investigation

4A. Literature Surveyed

The field of research which involves the study of selective surfaces for solar energy utilization is rapidly growing and has accumulated a significant body of research papers. In the past 10-20 years new journals dealing exclusively with solar energy applications have been started and have met with considerable success.[3] The conventional Engineering and Scientific journals also publish research results pertinent to solar energy applications. Some Journals have developed topical sections for publishing results in solar energy research.[4]

The Department of Energy (Formerly ERDA) publishes Energy Research Abstracts.[5] This publication abstracts publications on all phases of energy research including Solar Energy. Although the abstract service was started only in the past several years an effort was made to search earlier literature for information appropriate to the abstracting effort. This abstract service is an invaluable tool to the researcher entering the energy fields.

Part the effort of this contract was to explore the basic physics of selective absorbers and to understand the nature of their blackness. A similar effort was made in the appraisal of the use of infrared reflecting coatings on glass cover plates used in most flat plate solar collector designs. A consideration for the selective absorbers was to assess the information available on the basic theoretical physical description of their properties. While experimental data exists on a great variety of surfaces, there appears to be paucity of theoretical description.

In this section we will briefly summarize what conclusion we arrived at in examining the literature. We will not attempt to give an exhaustive summary as that

is done elsewhere[5]. Our effort was directed more at looking over the literature in conventional scientific journals[6] and covered several hundred papers in various fields.

4B. Theoretical Studies

A surface blackness in a given region of the spectrum is due to tbree general reasons: 1) absorption by internal modes (electrons, plasmons, phonons etc.) 2) surface roughness 3) interference. The first is treated in standard texts on solid state physics[7] and will only be discussed incidentally. The second category has received considerable attention in the literature. A practical case in point is that of "Gold Black". Gold black exhibits blackness from the ultraviolet to far in the infrared region of the spectra.[8] Zaeschrar and Nedoluka (ZN)[9] treat the optical properties of gold black using an equivalent circuit formulation and a Drude-Zener model for the complex dielectric function. They obtain some agreement with some of the samples reported by Harris.[8] The problem of the rough surface and its effects have been treated by a number of authors,[10-16] however there is little reference to materials utilized for solar energy applications. Several books on Solar Energy applications contain discussions on the basic properties of black absorbers.[18,19] These books also contain a great deal of experimental information on the various selective surfaces used for flatplate collectors. Ritchie and Window have calculated the properties necessary to make a graded-index single film solar absorbers.[17] Their results show a good absorber could be made with the right kind of material deposition on a metal substrate.

It is our conclusion that the theoretical understanding of selective surfaces in terms of fundamental physical properties is somewhat incomplete. The various effects contributing to selective blackness of absorber surfaces need to be better understood from a theoretical basis. The relative contributions and importance of surface roughness, internal electronic and lattice structure and interference effects needs to be determined. If this were accomplished it would be some-

what more direct to evaluate and parameterize proposed absorbing surfaces. The selection of materials for new surfaces would be facilitated if the parameterization of the properties in terms of basic physical quantities were available.

4C. Experimental Studies

The optical properties of gold black have been studied by several authors.[20,21] The importance of the particle size and film thickness on absorption properties are discussed. McKenzie[20] also studies the effect of oxygen and tungsten oxide on the selective absorption properties of gold-black. Although gold-black surfaces may not themselves be used as solar collectors, the understanding of gold-black serves as a useful model for understanding other systems.

Yamaguchi has studied the structural effects of copper black and platinium black.[22] He discusses the importance of the roughness of the surface in forming light traps and hence creating a non-reflecting surface.

New materials consisting of organic polymers have been reported in the recent literature as having selective properties.[23] This is a particularly attractive pursuit as the indications are that they would be inexpensive. Other new surfaces have been reported in the published literature and in unpublished contract reports. They are to numerous for us to attempt to list. This information is available in the Energy Abstracts in a concise and comprehensive form.

Another procedure that shows some promise for increasing the efficiency of that plate collectors is the coating of the cover plates with a suitable infrared reflector. Redaelli has reported on the reflectance properties of tin oxide films as glass in the infrared region.[24] If such a film could be made without substantially reducing the visible transmissions solar collector efficiency would be significantly improved.

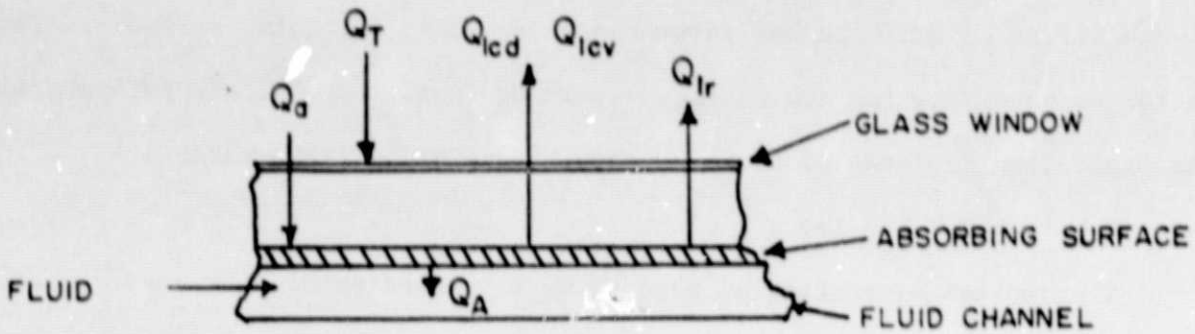

FLAT PLATE COLLECTOR

Figure 17a

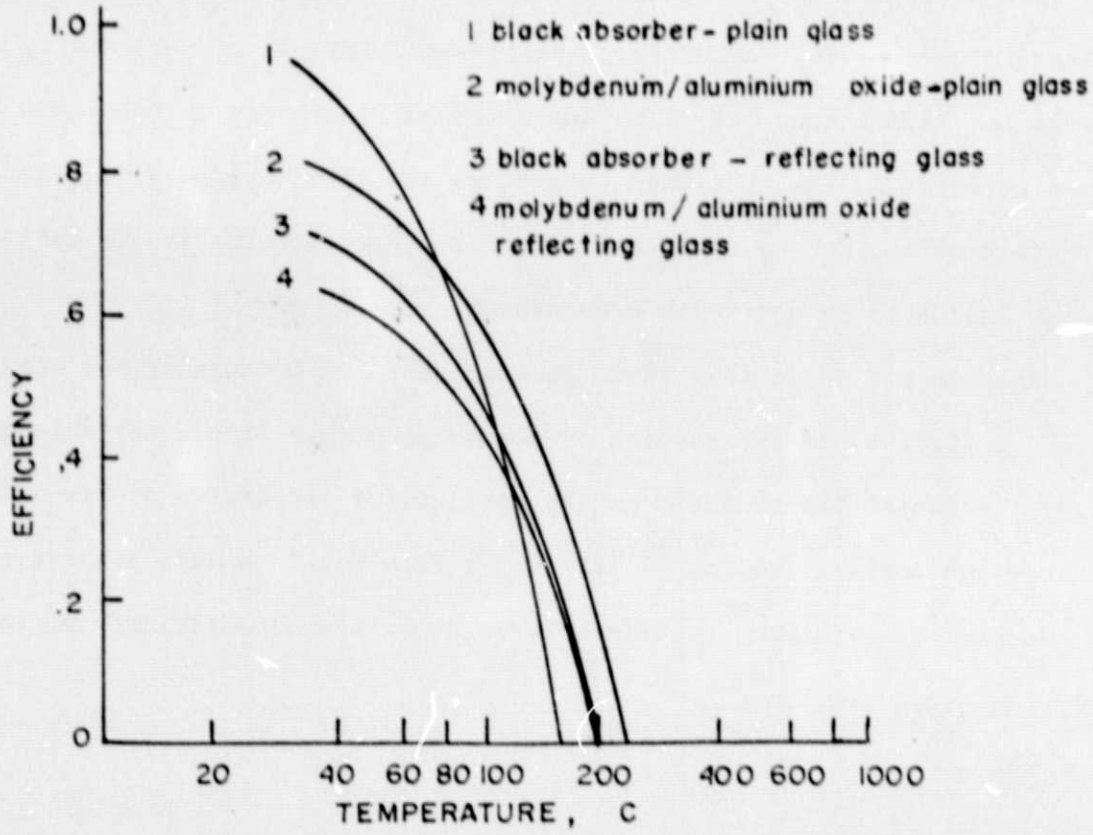

Figure 17b

5. Considerations for Collector Design:

Several authors[25-29] have recently reported calculations for the efficiencies of various types of solar energy collectors under varying conditions and with different types of cover plates and absorbing surfaces. While the details of the calculations and considerations differ somewhat, many of the results are in general agreement and are pertinent to some of the objectives of this project.

A diagram of a flat plate collector is shown schematically in Fig. 17a. The relevant heat flow parameters are given in the figure where:

Q_T = total incident flux

Q_A = heat absorbed by collecting fluid

Q_a = heat absorbed by absorbing surface

$Q_{\ell r}$ = heat loss by radiation

$Q_{\ell cd}$ = heat loss by conduction

$Q_{\ell cv}$ = heat loss by convection

This notation follows that given by Ahmadzadeh and Gascoigne[25] (AG). The efficiency of the collector is then defined by

$$\lambda = Q_A/Q_T \ .$$

The various authors treated the details of the calculation somewhat differently. (AG), for example, found an expression for Q_a in terms of an integral over radiation distributions and absorptivity as a function of wavelength. Young,[26] however, treats the problem in terms of average emissivity. In addition, the boundary conditions for the heat flow problem are handled differently.

The losses from the flat panel include radiation loss, conduction, and convective losses. The relative amounts of each loss is a function of temperature

and the details of the emissive properties. The loss of energy from the absorber to the glass cover plate is dominated at all temperatures by radiation, although convection and conduction play a part. The loss from the glass cover is dominated by convective losses for temperatures 50°C above ambient. The radiation loss is about constant[26] since the temperature of the cover plate does not depart too far from ambient temperature.

In terms of the parameterization given, the heat absorbed by the collecting fluid is

$$Q_A = Q_a - Q_{\ell r} - Q_{\ell cd} - Q_{\ell cv} .$$

Each of the heat loss terms, $Q_{\ell r}$, $Q_{\ell cd}$, and $Q_{\ell cv}$, can be calculated or estimated with varying degrees of sophistication. The degree of sophistication of these estimates is the primary difference in the model calculations performed. The results of (AG) for a black flat plate collector with a single plain glass window and with a reflecting window is shown in Figure 12B. Also shown are results for a selective surface, with two types of windows, one plain glass window and one coated to be infrared reflecting. At low temperature, i.e. less than 50°C above ambient (assumed to be 20°), the black absorber with a plain window exhibits a higher efficiency than the other models. It is only for temperatures in excess of 70°C that the selective absorber helps. It is further noted that a reflecting window does little good for either case at low temperatures. The results of Young show the same general trend. The solar absorptivity, α, of the surface is the dominant and most important parameter for low temperatures. It is more important to maintain a high α than to strive for a low infrared emissivity ε.

Dolan[5] experimentally determined the efficiency of a number of collector designs and surfaces both with a solar simulator and in actual solar absorbing conditions.

His results suggest the same thing, i.e. for low temperatures maintain a high α for optimal results.

Many of the applications of flat plate collectors will be for space heating and hot water supply where high temperatures will not be realized. For these applications it is probably best to optimize the solar absorptance for maximum efficiency. For similar reasons the use of reflecting cover glass plates needs to be carefully considered. By virtue of their reflectivity in the infrared region of the spectra the plates are somewhat less transparent to the solar radiation. This decreases the energy input to the absorbing plate and affects the overall efficiency. (AG) indicate, in fact, that reflecting coatings are counterproductive in most flat plate applications. If one is using a black absorber at high temperatures where radiation becomes important, it is better to go to a selective surface with plain glass than to add a reflecting glass cover plate to the plain black absorber.

The studies do indicate a need for selective surfaces in concentrating collectors. In these designs when the temperature of the absorber is in excess of 100°C the selective surface can significantly enhance the efficiency of the system.

If these observations concerning flat plate collectors are indeed found to be substantiated by further research, then efforts should be made toward producing durable black surfaces with high solar absorptance. The mechanical and weatherability criteria are then probably of greater importance than selectivity of the surface and should be optimized along with the solar absorptivity for cost effective and consumer attractable systems.

6. Other Lines of Investigation

This project was also interested in selective transmitting materials. While we have no conclusions we suggest investigation along the following lines:

1. Doping of thin oxide layers on glass as suggested by the data of Redaelli.[24]
2. Coatings of rare earth compounds on glass. In particular lanthanum hexaboride has very interesting properties.
3. Meshlike structures formed by large polymeric molecules such as teflon. If the mesh structure were of appropriate dimensions the window would act as a filter with selective properties.
4. Certain electro-optic materials such as potassium-dihydrogen phosphate have excellent selective transmission properties for solar applications. They also have the interesting feature that their optical properties are influenced by electric fields.

7. References

7. References

1. Helio Associates, Final Report-"Air Stable Selective Surfaces of Solar Energy Collectors",PB 252 505, NSF/RANN/SE/GI-41895/PR/74/7(1975).

2. e.g. O.S. Heavens, Optical Properties of Thin Solid Films, Butterworths, London (1955).

3. An example is The Journal of Solar Energy Science and Technology.

4. For example Journal of Applied Optics.

5. Available through the Department of Energy/Oak Ridge laboratories, Oak Ridge, Tennessee.

6. The following journals were examined for the past 12 years.

   a) Applied Optics

   b) Journal of the Optical Society of America

   c) Journal of the Electrochemical Society

   d) Chemistry Abstracts.

7. Also see J.C. Maxwell-Garnett, Phil trans. A 203, 385 (1904), Phil tran, A 205 237 (1906)

8. L. Harris,"The Optical Properties of Metal and Carbon Blacks." (The Eppley Foundation for Research, Newport R.I., Monograph Series No. 1, Dec. 1967).

9. G. Zaeschmar and A. Nedoluhy J.O.S.A. 62,340 (1971).

10. KE Torrance, and EM Sparrow J.O.S.A. 57, 1105 (1967)

11. R.W. Tokarskey and J.P. Morton J. App. Physics 79, 3051 (1974).

12. A.G. Emslie and O.R. Aronsoy, App. Optics 12 2563 (1973).
    A.G. Emslie and O.R. Aronsoy, App. Optics 12 2563 (1974).

13. Arthur L. Lathrop,JOSA 56, 926 (1966)

14. E. Kretchmann and E. Kroger, JOSA 65, 150 (1975).

15. J.O. Porteus, JOSA 53, 1394 (1963).

16. H.E. Bennett and J.O. Porteus JOSA 51, 123 (1961).

17. John Duffie and William Beckman, Solar Energy Thermal Processes, John Wiley, N.Y. (1914)

18. A.B. Meinel and M.P. Meinel, Applied Solar Energy, Addison-Wesley (1976)

19. I.T. Ritchie and B. Window, Appl. Optics 16, 1938 (1977)

20. D.R. McKenzie, JOSA 66, 249 (1976)

21. V.V. Truong and G.D. Scott, JOSA 66, 124 (1976)

22. S. Vamaguchi, Journal Electro Chemical Soc (Japan) 123, 1586 (1976)

23. D.F. Paul and R.W. Gumbs, J. Appl. Polymer Sci. 21, 959 (1977)

24. Giacomo Redaelli, Appl. Optics 15, 1122 (1976)

25. J. Ahmadzadeh and M. Gascoigne, Energy Conversion 16, 13 (1976).

26. M. Young, J. App. Optics 14, 1503 (1975).

27. F.L. Test, Energy Conversion 16, 23 (1976).

28. Rainer Köhne, "Der Flache Sonnenkollektor Energiebilanz and Wirkungsgrad," DLR-FB 75-3. Sponsored by Deutsche Forschungs and Versuchsanstalt für Luft and Raumfahrt.

29. F.J. Dolan, "A performance evaluation of various coatings, substrate materials and solar collector systems, " NASA-TM-X-73355, Sept. 1976.